bioRxiv preprint doi: https://doi.org/10.1101/2024.06.25.600597; this version posted June 29, 2024. The copyright holder for this preprint (which was not certified by peer review) is the author/funder, who has granted bioRxiv a license to display the preprint in perpetuity. It is made available under aCC-BY-ND 4.0 International license.

Supplemental Data Figures 1

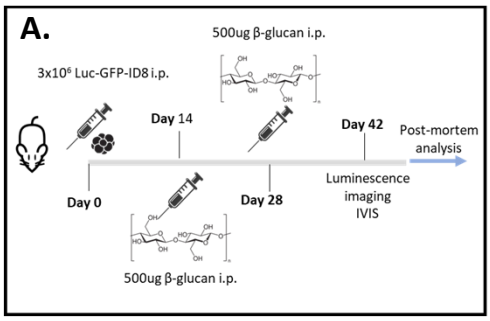

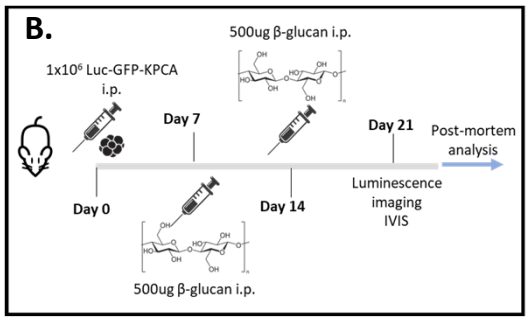

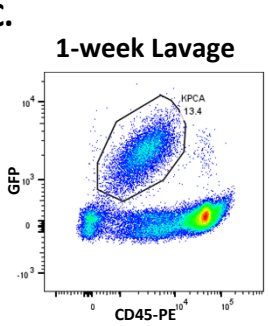

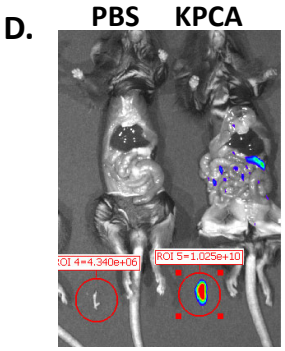

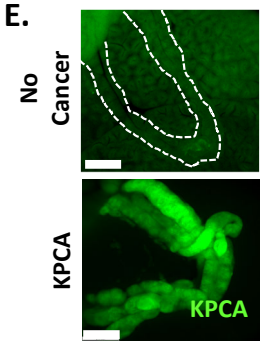

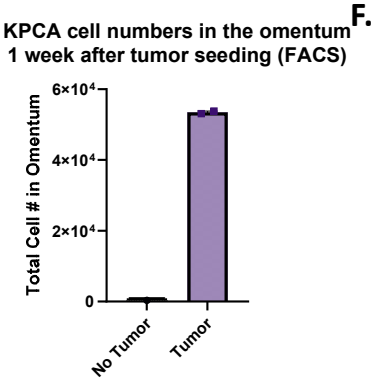

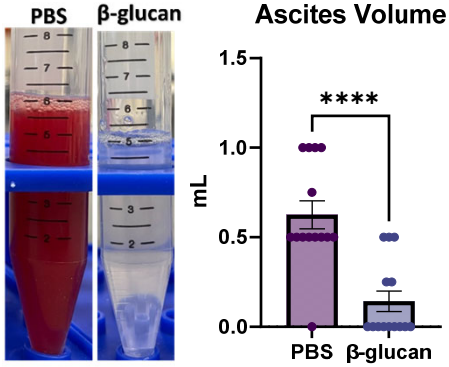

bioRxiv preprint doi: https://doi.org/10.1101/2024.06.25.600597; this version posted June 29, 2024. The copyright holder for this preprint (which was not certified by peer review) is the author/funder, who has granted bioRxiv a license to display the preprint in perpetuity. It is made available under aCC-BY-ND 4.0 International license.

Supplemental Data Figures 2

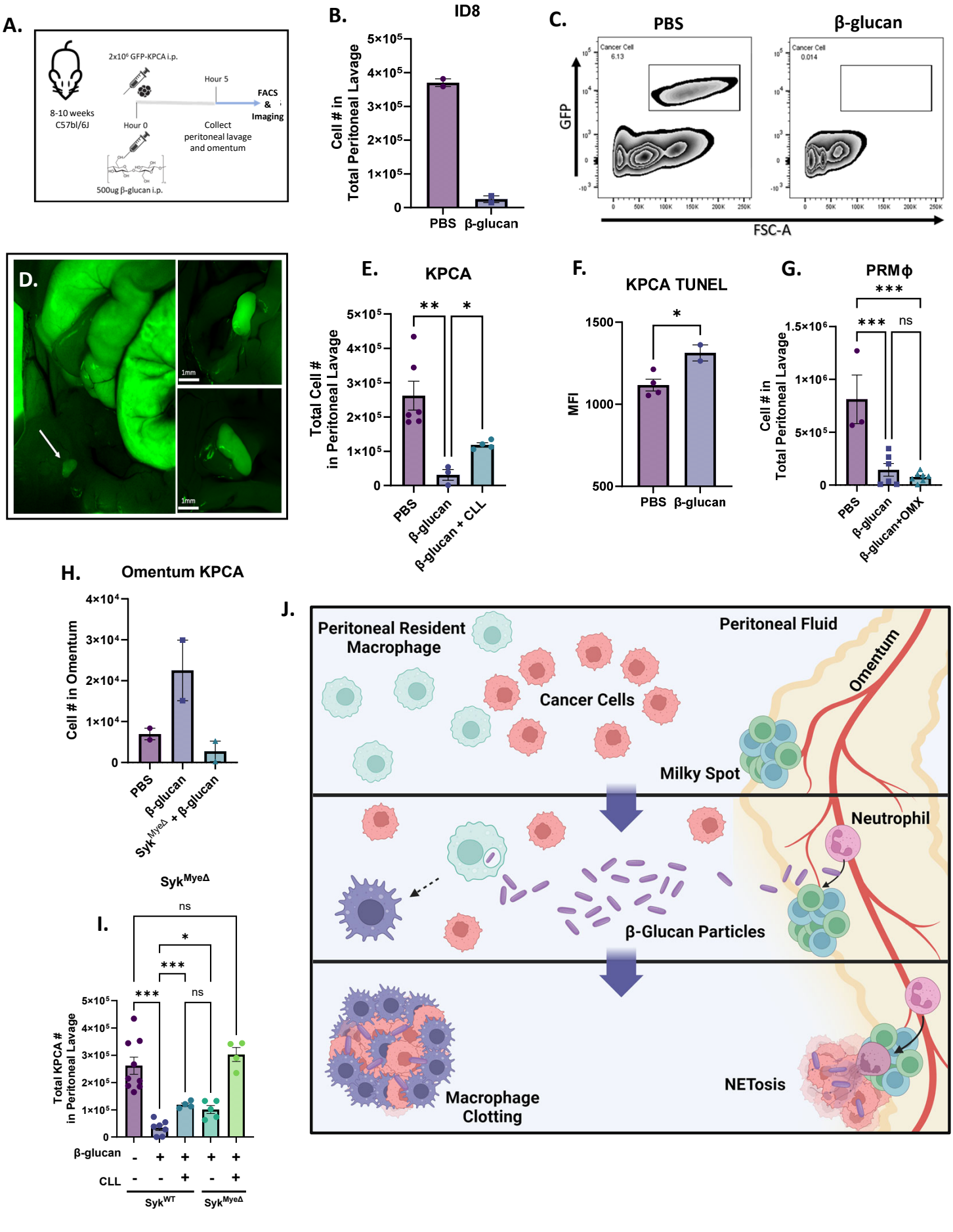

bioRxiv preprint doi: https://doi.org/10.1101/2024.06.25.600597; this version posted June 29, 2024. The copyright holder for this preprint (which was not certified by peer review) is the author/funder, who has granted bioRxiv a license to display the preprint in perpetuity. It is made available under aCC-BY-ND 4.0 International license.

Supplemental Data Figures 3

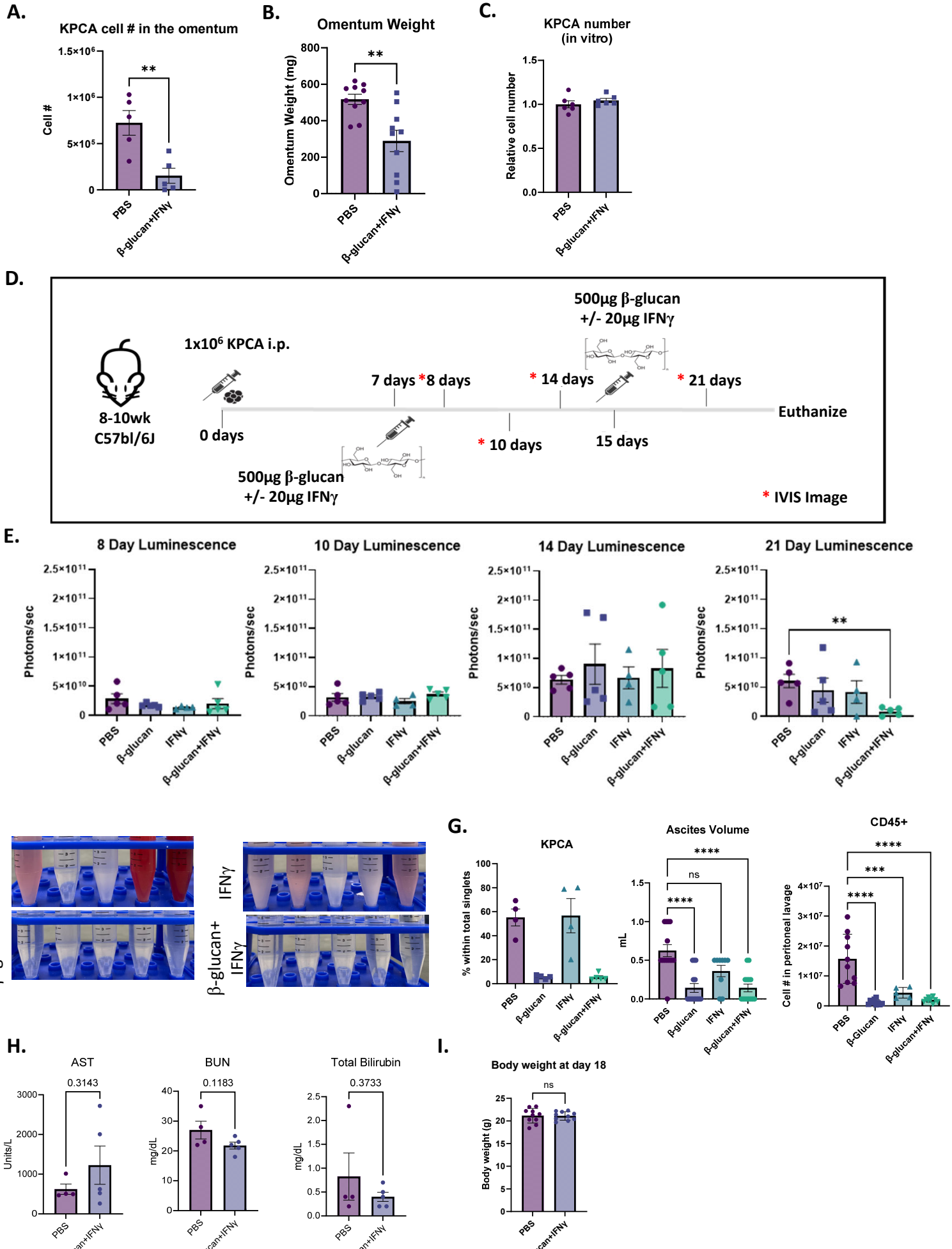

bioRxiv preprint doi: https://doi.org/10.1101/2024.06.25.600597; this version posted June 29, 2024. The copyright holder for this preprint (which was not certified by peer review) is the author/funder, who has granted bioRxiv a license to display the preprint in perpetuity. It is made available under aCC-BY-ND 4.0 International license.

Supplemental Data Figures 4

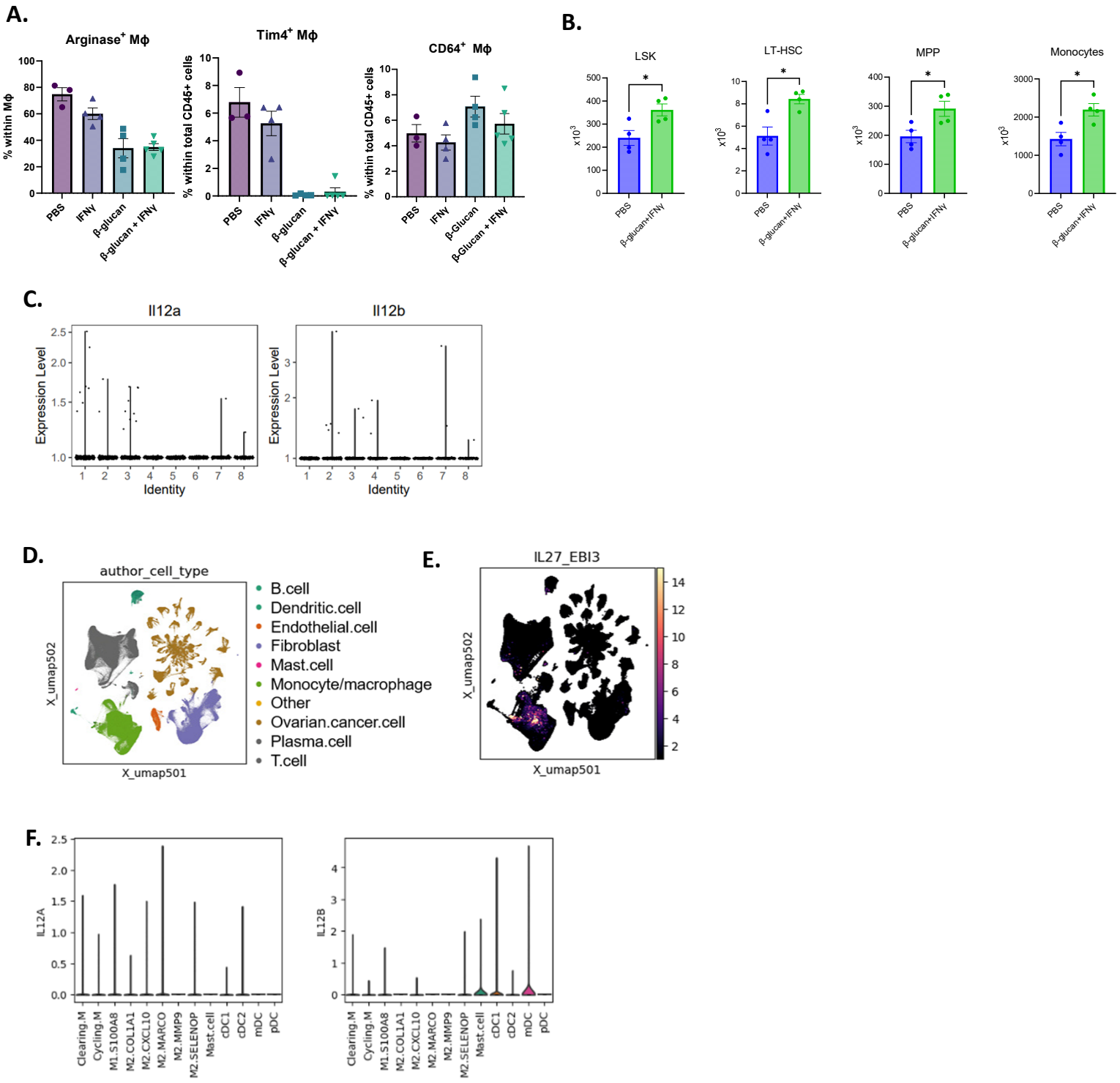

bioRxiv preprint doi: https://doi.org/10.1101/2024.06.25.600597; this version posted June 29, 2024. The copyright holder for this preprint (which was not certified by peer review) is the author/funder, who has granted bioRxiv a license to display the preprint in perpetuity. It is made available under aCC-BY-ND 4.0 International license.

Supplemental Data Figures 5

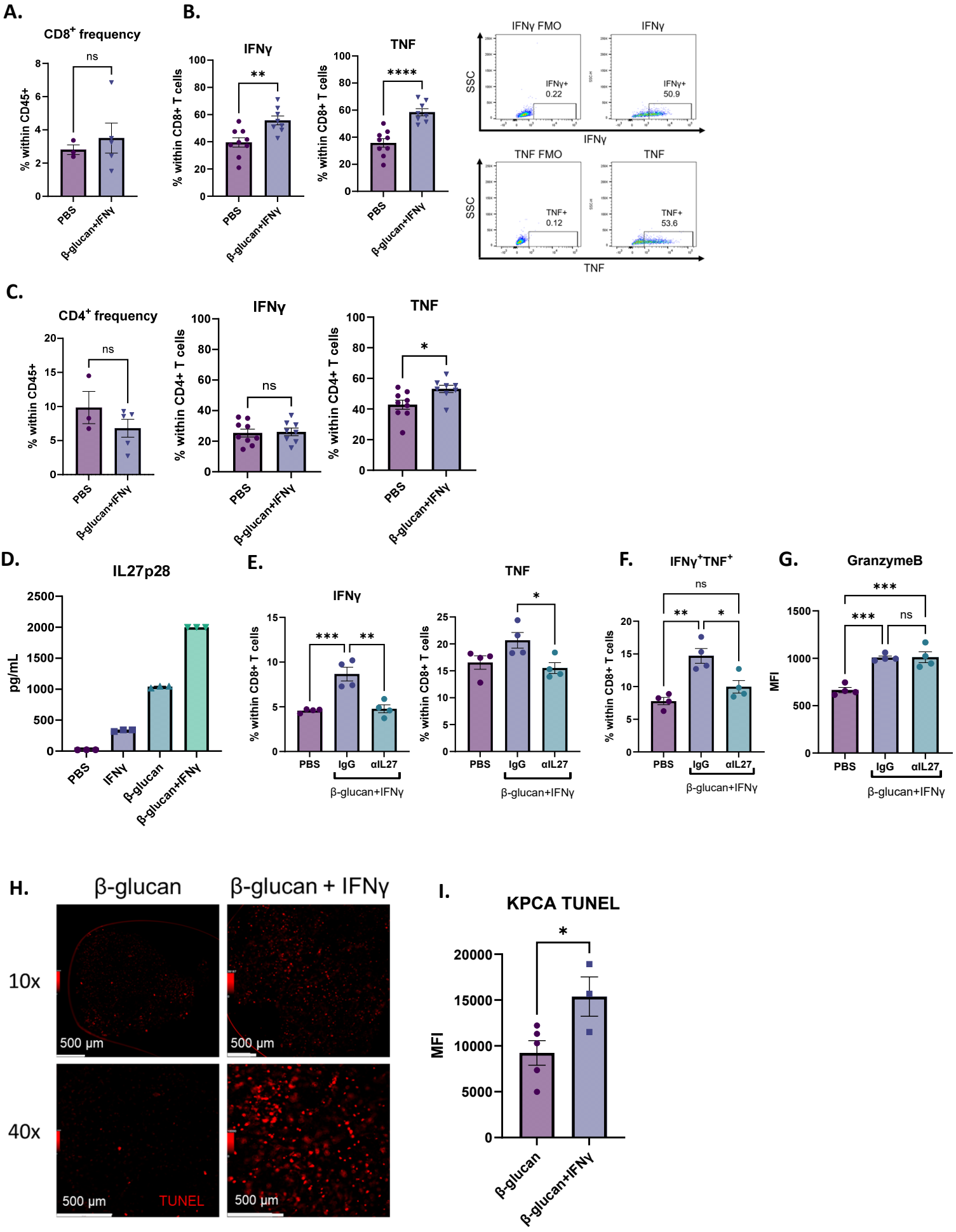

bioRxiv preprint doi: https://doi.org/10.1101/2024.06.25.600597; this version posted June 29, 2024. The copyright holder for this preprint (which was not certified by peer review) is the author/funder, who has granted bioRxiv a license to display the preprint in perpetuity. It is made available under aCC-BY-ND 4.0 International license.

Figure 4. BI enriched IL27+ macrophages in omentum tumors

(A) Whole body bioluminescence signals of PBS or CLL-treated mice treated with BI and control mice. (B) A UMAP plot of monocyte/MΦ clusters in omentum tumors. (C) Top expressed genes in all monocyte/MΦ clusters. (D) Frequencies of eight identified monocyte/MΦ clusters in omentum tumors. (E) Slingshot trajectory analysis from the origin (Cluster 5) through three independent pathways (red arrows). (F) qPCR analysis of Cluster 2-specific genes in monocyte-derived MΦs treated with PBS or BI. (G) Top upregulated IPA cytokine regulators in Clusters 1 and 2. (H) *Il27* and *Ebi3* co-expression heatmap in monocyte/MΦ clusters. (I) *Il27* expression in monocyte-derived MΦs treated with PBS or BI analyzed by qPCR. (J) UMAP monocyte/MΦ clusters and (K) *IL27* and *EBI3* co-expression in tumors from human OvCa patients. (L) Overall survival analysis in late stage OvCa patients (stage III and IV) with high and low co-expression of *IL27-EBI3.* Student's t test and log rank test were used. *p<0.05; **p<0.01; ****p<0.0001. Error bars are standard errors of the mean.

Figure 5. IL27 contributes to BI treatment by activating T cells and is specifically secreted by BI-stimulated MΦs.

(A) Bioluminescence signals of omentum tumors and (B) mesentery metastasis scores from mice injected with IgG or αIL27 treated with BI as well as PBS-treated control mice. (C) Mean fluorescent intensity (MFI) of IFNγ and TNF in $CD8^+$ T cells in omentum tumors from control or BI treated mice analyzed by flow cytometry. (D) ELISA quantification of IL27 heterodimer in supernatant from BMDM stimulated with PBS, IFNγ, β-glucan, or BI. (E) ELISA quantification of IL27 heterodimer in supernatant from WT-, $Syk^{Mye\Delta}$, Dectin-1 KO, and IFNγR KO BMDM cultured with PBS or BI. (F) IFNγ and TNF MFI of $CD8^+$ T cells cocultured with MΦ pretreated with PBS or BI in the presence of αIL27 antibody or control IgG. Student's t test and One-way ANOVA were used. *p<0.05; **p<0.01; ***p<0.001; ****p<0.0001. Error bars are standard errors of the mean.

Figure 6. BI extends overall survival in both chemoresistant and chemo-sensitive models and dramatically enhances chemotherapy response in the chemo-sensitive model.

(A) Survival curves of KPCA tumor-bearing mice treated with PBS, carboplatin, BI, or BI+carboplatin as indicated. The numbers of mice are PBS n=14, carboplatin n=10, BI n=20, BI+carboplatin n=15. The graph is a combination of three independent experiments. (B) survival curves of BPPNM tumor-bearing mice treated with BI and carboplatin as indicated. The numbers of mice are PBS n=14, carboplatin n=20, BI n=15, BI+carboplatin n=14. The graph is a combination of three independent experiments. Log-rank test was used.

Supplementary Figure 1.

Treatment timelines of (A) ID8 and (B) KPCA tumors treated with β-glucan. (C) Representative flow plot identifying GFP+CD45- KPCA cells in the peritoneal lavage of mice 1 week after tumor seeding. (D) Representative image and quantification of compartmental bioluminescent imaging. The omentum is removed from the cavity; signals (red circle) are obtained separately from the rest of the peritoneal cavity (non-omentum signal). (E) Representative fluorescent images of the omentum and KPCA numbers in the omentum of mice 1 week after KPCA cell injection. Scale bar is 2.5 mm. (F) Representative images of ascites and calculated changes in ascites volumes from PBS- or β-glucan-treated mice. student's t test was used. ****p<0.0001. Error bars are standard errors of the mean.

bioRxiv preprint doi: https://doi.org/10.1101/2024.06.25.600597; this version posted June 29, 2024. The copyright holder for this preprint (which was not certified by peer review) is the author/funder, who has granted bioRxiv a license to display the preprint in perpetuity. It is made available under aCC-BY-ND 4.0 International license.

Supplementary Figure 2.

(A) Acute cancer cell capture timeline. (B) Quantification of ID8 cells in the peritoneal lavage of mice 5 hours post β-glucan treatment. (C) Representative flow plots of GFP+ KPCA cells disappearing from the peritoneal lavage 5 hours after intraperitoneal β-glucan administration. (D) Representative *in situ* images of peritoneal clots formed in the peritoneal cavity after β-glucan treatment. These clots contain GFP+ KPCA cancer cells. (E) Quantification of KPCA cells in peritoneal lavage as determined by flow cytometry in control or CLL-pretreated mice 5 hours after intraperitoneal β-glucan administration. (F) MFI of TUNEL staining in KPCA cells in the clots β-glucan treated mice and peritoneal lavage from PBS-treated mice, which do not form clots. (G) Quantification of peritoneal resident macrophages (PRMΦs) in the peritoneal lavage of control or omentectomized (OMX) mice after β-glucan administration. (H) Quantification by flow of GFP+ KPCA cells in the omentum of Syk^{WT} and $Syk^{Mye\Delta}$ mice treated with β-glucan. (I) Quantification of KPCA cells in peritoneal lavage in Syk^{WT} and $Syk^{Mye\Delta}$ mice 5 hours post indicated treatment with PBS, β-glucan, or CLL. (J) Graphical representation of two mechanisms of cancer cell capture following intraperitoneal injection of β-glucan. One-way ANOVA and student's t test were used. *p<0.05; **p<0.01; ***p<0.001. Error bars are standard errors of the mean.

Supplementary Figure 3.

(A) KPCA cell numbers in the omentum evaluated by flow cytometry and (B) Omentum tumor weight in PBS- or BI-treated mice. (C) Quantification of KPCA numbers 48 hours following PBS and BI treatment *in vitro. S*tudent's t test was used. (D) Treatment and longitudinal imaging timeline in PBS-, IFNγ-, β-glucan-, and BI-treated mice. (E) Quantification of bioluminescence signals in mice tracked longitudinally from day 8 to day 21 after tumor seeding. (F) Representative images of ascites accumulation and (G) quantification of KPCA cells and CD45+ cells and ascites volumes based on the peritoneal lavage of mice treated with PBS, IFNγ, β-glucan, and BI 21 days after tumor seeding. (H) IDEXX clinical chemistry analyses of sera from PBS- or BI-treated mice. (I) Body weight of PBS- or BI-treated mice 18 days after tumor cell seeding. Student's t test and One-way ANOVA were used **p<0.01, ***p<0.001, ****p<0.0001. Error bars are standard errors of the mean.

Supplementary Figure 4.

(A) Quantification of frequencies of Arginase+ MΦs, Tim4+ MΦs, and CD64+ MΦs in omentum tumors treated as indicated and determined by flow cytometry. (B) Number of progenitor cells and monocytes in the bone marrow of mice 1 week after PBS or BI treatment. (C) Expression of *Il12a* and *Il12b* in monocyte/MΦ clusters pooed from mice treated with PBS, β-glucan, IFNγ, or BI. (D) UMAP plot of immune cells and co-expression of *IL27-EBI3* in human OvCa patient tumors. (F) Expression of *IL12A* and *IL12B* in each myeloid cell subclusters from human OvCa tumors. Student's t test was used. *p<0.05. Error bars are standard errors of the mean.

Supplementary Figure 5.

(A) Quantification of frequencies and (B) activation of $CD8^+$ T cells in omentum tumors from PBS- or BI-treated mic and flow cytometry plots of TNF- or IFNγ-stained samples, including fluorescence minus one (FMO) plots used to identify positive populations. (C) Quantification of frequencies and activation of $CD4^+$ T cells in omentum tumors from PBS- or BI-treated mice. (D) ELISA quantification of IL30 (IL27p28) in supernatant from BMDM cultured with PBS, IFNγ, β-glucan and BI. Frequencies of (E) IFNγ+ or TNF+, (F) IFNγ+TNF+ $CD8^+$ T cells, and (G)

bioRxiv preprint doi: https://doi.org/10.1101/2024.06.25.600597; this version posted June 29, 2024. The copyright holder for this preprint (which was not certified by peer review) is the author/funder, who has granted bioRxiv a license to display the preprint in perpetuity. It is made available under aCC-BY-ND 4.0 International license.

Granzyme B MFI of $CD8^+$ T cells cocultured with MΦ pretreated with PBS or BI in the presence of αIL27 antibody or control IgG. (H) Representative TUNEL staining in β-glucan- or BI-induced clots. (I) FACS quantification TUNEL MFI in GFP+ KPCA Cells. Student's t test and One-way ANOVA were used. *p<0.05; **p<0.01; ***p<0.001; ****p<0.0001. Error bars are standard errors of the mean.